Damage mechanisms identification of polymer based composite materials: time-frequency investigation of acoustic emission data based on Hilbert-Huang transform

S.E. Hamdi[a], A. Le Duff[a], G. Plantier[a], A. Sourice[a], L. Simon[b] and R. Feron[a]

[a]Groupe ESEO, rue Merlet de la Boulaye, 49009 Angers, France
[b]Laboratoire d'acoustique de l'université du Maine, Bât. IAM - UFR Sciences Avenue Olivier Messiaen 72085 Le Mans Cedex 9
seif-eddine.hamdi@eseo.fr

Presented in this paper, a time-frequency damage characterization procedure in Glass Fiber Reinforced Polymer (GFRP) composite materials based on the analysis of the Acoustic Emission (AE) signals by the Hilbert-Huang transform (HHT). It is to be noted that the study of damage by means of AE in polymer composites prompted the possibility of correlating a specific damage mechanism with its acoustic signature. Several studies highlighted the relevance of frequency spectral analysis in order to reconstruct the whole damage process. Thus, the assessment of the time-varying dominant frequencies present in a typical AE signal acquisition, can make easier the assessment of its structural damage potential. The main difficulty in defining a relationship between a specific damage mode and its acoustic signature is that the AE signals in GFRP materials are usually non-stationary and comprise overlapping transients. Signals of this kind require, first of all, a joint time-frequency analysis. In this context, the newly developed HHT is exclusively used in the present work for AE signals waveform analysis to describe the damage behavior as a first step for in situ detection of structural damages in polymer based composite materials.

1 Introduction

In the last decade, Glass fiber reinforced polymer (GFRP) composite materials has been extensively used for numerous industrial applications. despite their attractive mechanical behavior,their damage mechanisms still require a better understanding. Several studies [1, 2] highlighted the performance of the Acoustic Emission (AE) technique for in situ health monitoring applications in composite materials. A key part of the analysis aims then to identify the most relevant descriptors of critical damage mechanisms occurring in these materials.

Recently, the Hilbert-Huang Transform (HHT) [4, 6, 7], has been applied for non-stationary signals features analysis. Peng et al. [3] shows that the HHT can provide a relevant descriptors for both analysis and features extraction of vibration signal. In this paper, the HHT is used for the extraction of a damage mechanisms features from AE signals in polymer composite materials. Hence, as a first step to a possible application to monitoring damage growth in GFRP structures, this technique is applied on a well-controlled tests with typical sources of AE signals. Unidirectional GFRP composites samples are studied. First, the acquisition of the AE signals is performed thanks to a wide-band acoustic transducer. Then, the HHT is used to identify the damage signature, by correlating the measured AE signals with a well-established acoustic sources.

The paper is structured as follows: In section 2, the principle of the HHT is presented. In section 3, describes the experimental procedure. The AE signals HHT based features extraction and results are discussed in section 4. Lastly, in section 5, some conclusions and future work is initiated.

2 Principle of the HHT

The HHT, developed by Huang et al. [4, 5, 6, 7], is a time-frequency signal processing technique which was specially designed to analyze non-stationary data changes even within one oscillation cycle [8]. This method tends to empirically extract the intrinsic oscillation modes by their characteristic time scales in the data, and then to decompose the data accordingly.

2.1 EMD method

The EMD decomposes signals into a set of intrinsic mode functions (IMFs) which represent simple oscillatory modes. Generally, the finest component of the shortest period at each instant will be identified and decomposed into the first IMF. The components of longer periods will be identified and decomposed into the following IMFs in sequence [9, 10]. The EMD method is based upon the assumption that any signal is composed from the contribution of different IMFs. For each one, it will assigned the same number of extrema and zero-crossings. There is only one extremum between successive zero-crossings. Each IMF should be independent of the others. In this way, each signal could be considered as the sum of a finite IMFs components, each of which must satisfy the following definition [5, 6, 7]:

1. In the whole data set, the number of extrema and the number of zero-crossings must either equal or differ at most by one;

2. At any point, the mean value of the envelope defined by local maxima and the envelope defined by the local minima is zero.

The EMD decomposes data in a few steps. Hence, any signal $x(t)$ can be decomposed as follows [7]:

1. Identification of all the local extrema, then connecting all the local maxima by a cubic spline line as the upper envelope.

2. Repeating the same process for the local minima to produce the lower envelope. The upper and lower envelopes should cover all the data between them.

3. The mean value of upper and lower envelope is designated as m_1, and the difference between the signal $x(t)$ and m_1 is the first component, h_1, (see Figures 1 and 2). In that way, we have

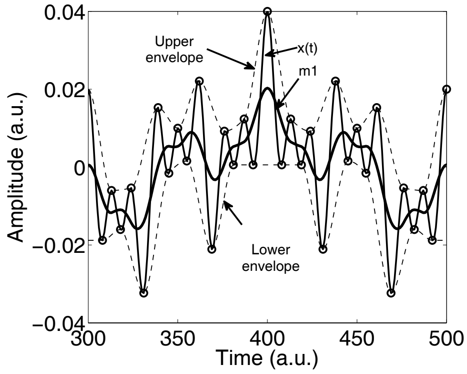

Figure 1: Sifting process: the original data $x(t)$ with the upper, lower envelope (dotted lines) and resultant mean line m_1 (bold line).

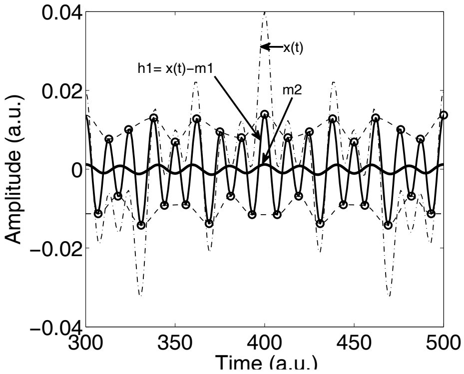

Figure 2: The data after the first sifting process.

$$x(t) - m_1 = h_1. \tag{1}$$

If h_1 satisfy the IMF requirements, then h_1 can be considered as the first component of $x(t)$.

4. If h_1 is not an IMF, it is treated as the original signal and repeat the steps 1-3; then

$$h_1 - m_{11} = h_{11}, \tag{2}$$

where, m_{11} is the mean of both upper and lower envelope value of h_1. This procedure is called sifting process and is repeated, up to k times, on the successive data h_{ik} until the mean line between the upper and lower envelopes is near zero for any point. Then,

$$h_{1(k-1)} - m_{1k} = h_{1k}, \tag{3}$$

and the first IMF component, designated as

$$c_1 = h_{1k}, \tag{4}$$

represents the finest scale or the shortest period component of the signal $x(t)$.

5. Extracting c_1 from $x(t)$, leads to:

$$r_1 = x(t) - c_1. \tag{5}$$

The whole sifting process is repeated on r_1, for n times, to obtain the successive components of increasing period. Then n IMFs of signal $x(t)$ could be obtained. Hence,

$$r_{n-1} - c_n = r_n. \tag{6}$$

When r_n becomes a monotonic function from which no more IMF can be extracted, then the decomposition process can be stopped. By cumulating (5) and (6)

$$x(t) = \sum_{j=1}^{n} c_j + r_n, \tag{7}$$

where the last component r_n, treated as a residue, is the mean trend of $x(t)$. The IMFs $c_1, c_2, \ldots, c_n$ include different frequency bands ranging from high to low. The frequency components contained in each frequency band are different and they change according to the variation of signal $x(t)$.

An IMF is a counter part to the simple harmonic function, but it is much more general: instead of constant amplitude and frequency, IMFs can have both variable amplitude and frequency as functions of time. This frequency-time distribution of the amplitude is designated as the Hilbert amplitude spectrum, or simply the Hilbert spectrum. Now, the next section deal with the Hilbert spectrum analysis.

2.2 Hilbert spectrum analysis

The Hilbert spectrum analysis provides a method for considering instantaneous frequency, which can be used for an accurate investigation of composite structures [11]. One of the easiest way to calculate the instantaneous frequency, $F_{i_{x(t)}}(t)$, is to apply the Hilbert transform. Indeed, for a real signal $x(t)$, it is possible to use the analytic signal $z(t)$ associated to $x(t)$,

$$z(t) = x(t) + jy(t) = a(t)\exp\left[j\theta(t)\right], \tag{8}$$

in which,

$$a(t) = \sqrt{x^2(t) + y^2(t)}, \tag{9}$$

$$\theta(t) = \arctan\left[\frac{y(t)}{x(t)}\right]. \tag{10}$$

From equation 10, we can have the instantaneous frequency as

$$F_{i_{x(t)}}(t) = \frac{1}{2\pi}\frac{d\theta(t)}{dt}. \tag{11}$$

After performing the Hilbert transform to each IMF component, the original time-series $x(t)$, can be expressed as the real part (RP) of $z(t)$:

$$x(t) = \sum_{i=1}^{n} a_i(t)\exp\left[j2\pi F_{i_{x(t)}}(t)t\right]. \tag{12}$$

In equation 12, both amplitude, $a_i(t)$ and frequency $F_{i_{x(t)}}(t)$ of each component are presented as functions of time. This time-frequency distribution of the amplitude is designated as the Hilbert spectrum (HS). Various forms of Hilbert spectra presentations can be made [7]. The Marginal Hilbert Spectrum (MHS), offers a measure of total energy contribution from each frequency value, i.e the MHS represents the cumulated amplitude over the entire data span [5, 7]. If more qualitative results are desired, the smoothed presentation of the Hilbert spectrum is preferred. In the smoothed form, the energy density and its trends of evolution as functions of frequency and time are easier to identify. Several smoothing methods can be applied [5]. In this work, a 15 × 15 weighted Gaussian filter will give the Smoothed Hilbert Spectrum (SHS).

3 Experimental set-up and procedures

3.1 Samples description

The experimental procedure is carried out on GFRP composite materials. Rectangular samples of unidirectional fiber-matrix composites are obtained by a hand lay up technique in the lab. Quasi-static three points bending tests are performed as shown in figure 3. These tests are well established procedures and gives rise to specific damage mechanisms from their AE signals [12, 13]. According to those previous studies, matrix cracking (A signals) and matrix/fiber debonding (B signals) caused the F45 samples failure. The samples are loaded with a loading direction at 45° according to the fiber direction. In that way, no fiber breaking is initiated. In order to generate typical fiber breakage (C signals), and delamination (D signals) AE signals, quasi-static three points bending tests are performed on F0 unidirectional composite samples. In this case, F0 samples are loaded with a loading direction at 0° according to the fiber direction.The type of tests, the lay-ups used, the abbreviated names, and the visually reported damage mechanisms for each sample used in the rest of the paper, are given in table 1. The geometry of each sample and the sensors location are given in table 2.

3.2 AE acquisition set-up

In order to let the AE signals be continuously recorded, a PXI® (PCI eXtensions for Instrumentation) manufactured by National Instrument [14], is used. Two piezoelectric sensors were mounted on the GFRP samples as shown in figure 3, and secured with small clamps. The sensors used are a broadband sensors with an operating frequency range lying from 100 kHz to 1 MHz. The acquired signals are first pre-amplified with a 40 dB pre-amplification, and then high-pass filtered with a 100 kHz cutoff frequency. The AE signals are then digitized and stored with the PXI® system. The trigger circuitry was set to 0.2 mV threshold in order to save discret AE waveforms. The system triggers when the signal on any channel exceeds the threshold and then records data on the two channels. 1024 points per waveform are recorded at a 5 MHz sampling rate. The AE data acquisition stops when final failure occurred. The test setup (see figure 4) shows the GFRP specimen with the two sensors, preamplifiers, and the AE data acquisition system.

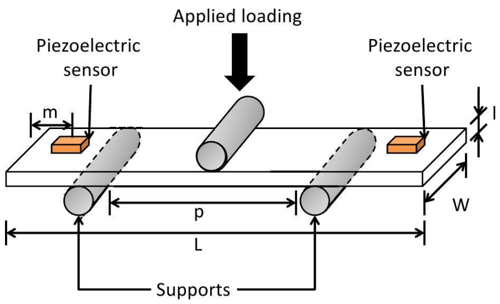

Figure 3: Samples geometry, sensors location, and loading set.

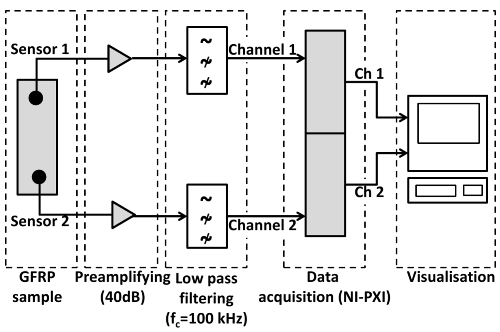

Figure 4: AE acquisition equipment.

4 Results and discussion

4.1 Damage characterization: HHT based analysis of F45 AE data

Typical A (matrix cracking), and B (matrix/fiber debonding) waveforms for the F45 composite samples under bending tests are presented, in figures 5 and 6. A signals waveforms are characterized by much shorter rise time, shorter duration and lower amplitudes and energies then B signals waveforms. The HHT based analysis is first validated on these two signals.

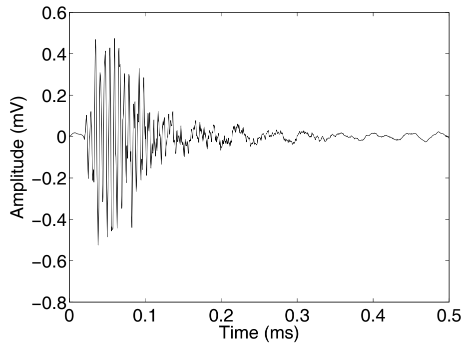

Figure 5: Matrix cracking (A signal).

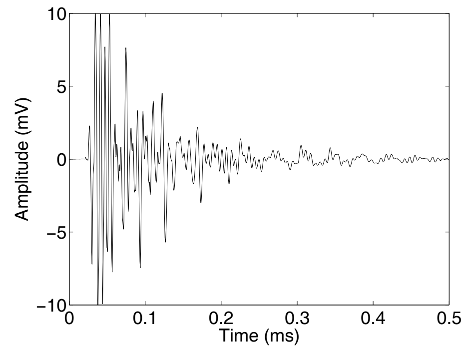

Figure 6: Matrix/fiber debonding (B signal).

The HHT is performed on the typical A and B signals identified above. A first qualitative interpretation of the time-frequency representations of both signals by SHS (see figures 7 and 8), shows high energy areas (high instantaneous amplitude levels) which corresponds to the frequency signature of both matrix cracking (see figure 7) and matrix/fiber debonding (see figure 8). Both damage mechanisms shows stretched energies distribution on the entire waveforms. Although, the peak of these time-frequency distributions is easily selected. Matrix cracking shows local peaks frequencies located around 100 kHz, and around 180 kHz for matrix/fiber debonding.

4.2 Damage characterization: HHT based analysis of F0 AE data

After AE signals are obtained, typical C (fiber breakage), and D (delamination) signals for the F0 samples are selected. C signals waveforms (see figure 9), are characterized by much shorter rise time, shorter duration and higher

Table 1: Type, layup and resulting damage modes of tests

Type of test	Layup	Number of specimens	Label	Reported damage mechanisms
Bending test	$[45^{\circ}]_{12}$	5	F45	Matrix cracking and matrix/fiber debonding
Bending test	$[0^{\circ}]_{8}$	5	F0	Fiber breakage and delamination

Table 2: Bending samples geometry

samples label	L (mm)	W (mm)	l (mm)	m (mm)	p (mm)
F45	280	20	3	25	100
F0	200	20	2	25	100

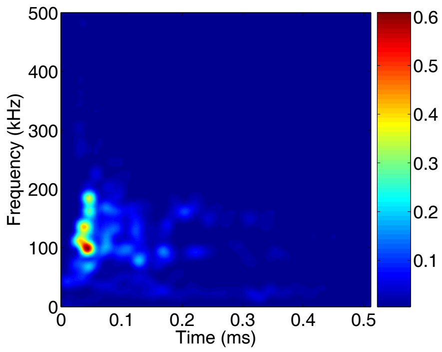

Figure 7: SHS of matrix cracking (A signal).

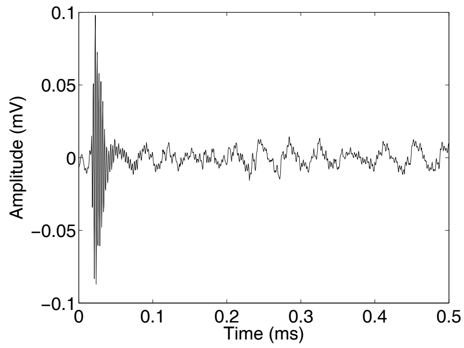

Figure 9: Fiber breakage (C signal).

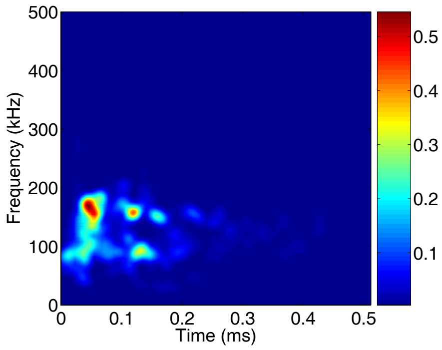

Figure 8: SHS of matrix/fiber debonding (B signal).

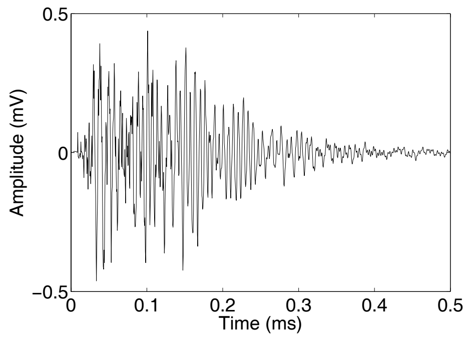

Figure 10: Delamination (D signal).

energies then D signals waveforms (see figure 10). The HHT based analysis is then performed on these two signals.

The time-frequency representations of both typical damage mechanisms waveforms by SHS, shows high energy areas which corresponds to the frequency signature of both fiber breakage (see figure 11) and delamination (see figure 12). Fiber breakage shows very local energies distribution at the beginning of the C waveforms, and located at higher frequencies (around 400 kHz), then delamination (around 80 kHz) which energy contribution seems to be stretched on the entire waveforms.

5 Conclusion

A time-frequency based on HHT analysis was performed on typical waveforms conventionally reported to be the temporal signature of damage mechanisms on GFRP composites. This procedure shows a possible discrimination between the different damages signature based on their peak frequencies estimation. The HHT provide encouraging results for non-stationary AE signals features extraction. This paper opens new perspectives, work on the instantaneous frequencies signals content may provide relevant damage descriptors for in situ health monitoring applications.

References

[1] T. Uenoya. "Acoustic emission analysis on interfacial fracture of laminated fabric polymer matrix composites" *Journal of Acoustic Emission* **13** 95-102, (1995)

[2] R. B. Clough, W. McDonough, "The measurement of fiber strength parameters in fragmentation tests by using acoustic emission" *Composites Science and Technology* **56** 1119-1127, (1996)

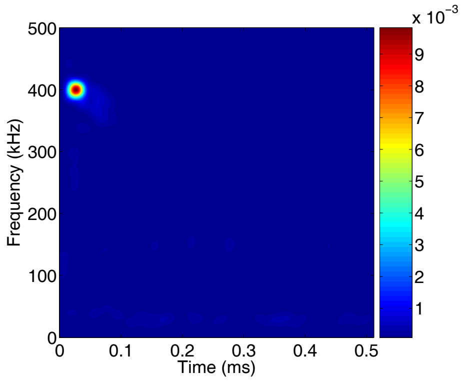

Figure 11: SHS of fiber breakage (C signal).

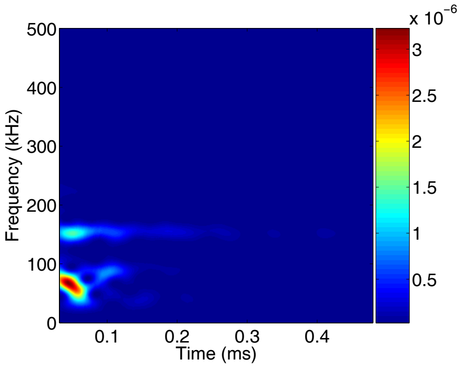

Figure 12: SHS of delamination (D signal).

[3] Z. Peng, P. Tse, F. Chua, "An improved Hilbert-Huang transform and its application in vibration signal analysis" *Journal of Sound and Vibration Volume* **286** 187-205, (2005)

[4] N. E. Huang, S. R. Long, Z. Shen. "The mechanism for frequency down-shift in nonlinear wave evolution", *Advances in Applied Mechanics* **32**, 59-117, (1996)

[5] N. E. Huang, Z. Shen, S. R. Long, M. C. Wu, H. H. Shih, Q. Zheng, N. C. Yen, C. C. Tung, H. H. Liu, "The empirical mode decomposition and the Hilbert spectrum for nonlinear and non-stationary time series analysis", *Proceedings of the Royal Society A Mathematical Physical and Engineering Sciences* 903-995, (1998)

[6] N. E. Huang, Z. Shen, S. R. Long, "A new view of nonlinear water waves: The Hilbert spectrum", *Annual Review of Fluid Mechanics* **31**, 417-457, (1999)

[7] N. E. Huang, "Introduction to the Hilbert-Huang Transform and its related mathematical problems", *Hilbert-Huang Transform and its applications* 324-331, (2005)

[8] R. Kazys, O. Tumsys, D. Pagodinas, "Ultrasonic detection of defects in strongly attenuating structures using the Hilbert-Huang transform", *NDT &E International* **41**, 457-466, (2008)

[9] C. C. Lin, P. L. Liu, P. L. Yeh, "Application of empirical mode decomposition in the impact-echo test", *NDT &E International* **42**, 589-598, (2009)

[10] S. Loutridis, E. Douka, L. J. Hadjileontiadis, "Forced vibration behaviour and crack detection of cracked beams using instantaneous frequency", *NDT &E International* **38**, 411-419, (2005)

[11] L. Lin, F. Chu, "Feature extraction of AE characteristics in offshore structure model using Hilbert-Huang transform", *Measurement* **44**, 46-54, (2011)

[12] S. Huguet, *Application de classificateurs aux données d'émission acoustique: identification de la signature acoustique des mécanismes d'endommagement dans les composites ŕ matrice polyère*. Thèse de Doctorat, Institut National Des Sciences Appliquées de Lyon, 153, (2002)

[13] A. Marec, J. H. Thomas, R. El Guerjouma, "Damage characterization of polymer-based composite materials: Multivariable analysis and wavelet transform for clustering acoustic emission data", *Mechanical Systems and Signal Processing* **22**, 1441-1446, (2008)

[14] National Instruments Corporation. NI PXI-1045 User Manual. p63, (2005)